Journal of Power Sources 224 (2013) 202–210

Contents lists available at SciVerse ScienceDirect

Journal of Power Sources

journal homepage: www.elsevier.com/locate/jpowsour

Formation of an integrated catalyst-coated membrane using electrohydrodynamic atomization Layer-by-Layer deposition for direct methanol fuel cells

Dazhi Wang [a,b,*], Liang Wang [a], Junsheng Liang [a,b], Zhangxun Xia [c], Suli Wang [c], Yingli Zhu [d], Chong Liu [a,b], Gongquan Sun [c]

[a] Key Laboratory for Micro/Nano Technology and System of Liaoning Province, Dalian University of Technology, Dalian 116024, China
[b] Key Laboratory for Precision and Non-traditional Machining Technology of Ministry of Education, Dalian University of Technology, Dalian 116024, China
[c] Dalian Institute of Chemical Physics, Chinese Academy of Sciences, Dalian 116023, China
[d] School of Mechanical Engineering, Tianjin University of Science and Technology, 300222 Tianjin, China

HIGHLIGHTS

- An integrated CCM was prepared using EHDA LbL deposition.
- The cathode of integrated CCM still presented compact feature after the life test.
- The 3 M methanol concentration gave the highest cell performance.
- The increase level of the cell performance decreased at higher temperature range.

ARTICLE INFO

Article history:
Received 23 May 2012
Received in revised form
25 September 2012
Accepted 27 September 2012
Available online 10 October 2012

Keywords:
Direct methanol fuel cell
Catalyst-coated membrane
Electrohydrodynamic atomization
Layer-by-Layer deposition

ABSTRACT

In this work, an integrated catalyst-coated membrane (CCM) is prepared by successively spray deposit Pt/C nano-suspension, Nafion solution and Pt–Ru/C nano-suspension on a cathode gas diffusion layer using electrohydrodynamic atomization (EHDA) Layer-by-Layer (LbL) deposition. Porous cathode and anode catalyst layers and dense Nafion membrane are deposited using the EHDA LbL deposition technique. It is also found that the EHDA LbL deposited CCM presents close packed structure. An 85 h life test shows that the EHDA LbL deposited cathode electrode side of the integrated CCM still presents well compact feature. Whereas, the delamination of the anode electrode side formed by direct pressing method is evident. The performance of the cell with different methanol concentrations is also examined. It is found that the 3 M methanol concentration gives the highest cell performance. Moreover, the polarization behaviour, methanol crossover and impedance response of the cell at different working temperatures are analysed. The cell performance demonstrates faster increase between 20 °C and 50 °C than between 50 °C and 70 °C. The methanol crossover test shows that the cell presents higher increase level of methanol crossover between 40 °C and 50 °C than other 10 °C temperature increase steps.

1. Introduction

Direct methanol fuel cells (DMFCs) have attracted considerable attention as an alternative power source for portable electronic devices such as cellular phones and laptops owing to their potential of high energy density, simple system configuration and low operating temperature [1–3]. In DMFC systems, the membrane electrode assembly (MEA) plays a key role, which consists of gas diffusion layers (GDLs), catalyst layers (CLs) and a polymer electrolyte membrane (PEM). MEA fabrication methods can be mainly categorized based on the substrate type used for the catalyst coating process, in which the catalyst could be coated either onto a gas diffusion layer (GDL-based MEA) or directly onto an electrolyte membrane (CCM-based MEA) [4,5]. It is reported that the MEA prepared by the CCM method provides better power density due to an extended catalyst/ionomer interface and improvement of catalyst utilization [6].

In the CCM method, the CLs are normally applied to both sides of the PEM by spraying [7], painting [8] and catalyst decaling [9]. The

* Corresponding author. Key Laboratory for Micro/Nano Technology and System of Liaoning Province, Dalian University of Technology, Dalian 116024, China. Tel.: +86 (411)84707949/2171; fax: +86 (411)84707940.
E-mail address: d.wang@dlut.edu.cn (D. Wang).

0378-7753/$ – see front matter © 2012 Elsevier B.V. All rights reserved.
http://dx.doi.org/10.1016/j.jpowsour.2012.09.092

CLs and PEM are usually treated as individual elements during fabrication using the above methods. The delamination of CLs from PEM usually happens during repeated working process due to the low bonding energy between them [10], which can reduce the catalytic efficiency. In addition, the structure features, including particle size, particle arrangement and porosity of the CLs are difficult to control using the above fabrication methods due to the thick single layer coating and controlling difficulty of fabrication process [11], which consequently cannot adequately match the requirement of the CLs in DMFC.

Layer-by-Layer (LbL) deposition of multilayered ultra thin films in a simple way is considered as a promising and efficient method for the preparation of CCM [12]. A major advantage gained from LbL technique is the introduction of a large number of variables that can modify the CLs depending on the experimental conditions. Recently, this deposition method has attracted a number of researchers' attention [13–15]. Electrohydrodynamic atomization (EHDA) is a method capable of controlling deposition of nano-structures LbL via different working parameters, which makes it possible to provide a new way for forming CCM. EHDA is a physical process that makes use of electrical and mechanical forces to form a liquid jet and its further disintegration into droplets [16], which was first reported by Zeleny in 1914 [17]. The atomizer nozzle is usually made in the form of a metal capillary into which liquid or suspension can be pumped. Depending on the requirement of droplets/relics motion a plate, ring or point (positioned below the nozzle) is served as the ground electrode [18,19]. According to the geometry of the jet and droplet, the resulting atomization modes can be mainly classified as dripping, microdripping, spindle, multi-spindle, cone-jet and multi-jet [20]. Among these modes, the cone-jet mode, which is the steadiest mode of spraying, can regularize the break-up of the jet to generate fine and uniform droplets/relics ranging from micrometres to nanometres in size. Liquids are initially used in the process of EHDA, and the investigations on it are comprehensive [21,22]. The use of suspension and nano-suspension in EHDA is a more recent development [23,24]. The distinct advantages of this technique with the use of suspensions include its capability of forming fine and controllable deposition products and less risk of nozzle blockage during processing which is frequently observed with other droplet forming routes such as piezo-head drive ink-jet printing [25]. Moreover, droplets/relics formed by EHDA are charged, which can self-disperse in space, resulting in the absence of droplet coagulation [26]. This technique has shown great potential in recent years and has been introduced to produce nano-particles [27], deposit thin films [28] and direct writing micro-structures in bioengineering and chemical engineering [29,30].

In this work, an integrated CCM was prepared using the EHDA LbL deposition. The well dispersed and stable Pt/C nano-suspension, Nafion solution and Pt–Ru nano-suspension were prepared and atomize-deposited successively using the EHDA LbL deposition technique to form all components of the CCM. During the EHDA deposition the atomization characteristics of Pt/C and Pt–Ru/C nano-suspensions and Nafion solution and the deposited films of anode and cathode CLs and Nafion membrane were examined. The performance and life test of the integrated CCM were also studied.

2. Experimental

2.1. Catalyst suspensions and Nafion solution

The anode and cathode catalyst suspensions used to prepare the CLs using EHDA LbL deposition are Pt/C and Pt–Ru/C nano-suspensions. The Pt/C nano-suspension was prepared by first mixing 1.5 g of distilled water and 0.05 g of Pt/C catalyst powder (40 wt.%, Pt particle size ~4.5 nm, Johnson Matthey Plc, London, UK) by magnetic stirring for 10 min. Then 1.5 g of ethanol (99.7 wt.%, Tianjin Kermel Chemical Reagent Co., Ltd, Tianjin, China) and 0.1 g of Nafion solution (5 wt.%, DuPont, Wilmington, USA) was added and mixed under ultrasonic bath for 2 h. The Pt–Ru/C nano-suspension was prepared by first mixing 0.5 g of distilled water and 0.05 g of Pt–Ru/C catalyst powder (60 wt.%, Pt–Ru particle size ~6 nm, Johnson Matthey Plc, London, UK) by magnetic stirring for 10 min. Then 1 g of ethanol and 0.15 g of Nafion solution were added and mixed under ultrasonic bath for 2 h.

The addition of Nafion solution was to stabilize the suspensions and to increase the hydrophilic property of CLs, which can increase the transport ability of the electrochemical reaction products in fuel cells [31]. The use of ethanol as liquid carrier was due to its easy volatilization behaviour, which can simplify the drying process of the CLs. Spontaneous combustion can occur in the presence of concentrated, finely dispersed catalyst (Pt/C and Pt–Ru/C nano-particles) and organic solvents such as ethanol in atmosphere environment. The Pt/C and Pt–Ru/C nano-particles can lose their activity. Therefore, the distilled water was mixed with Pt/C or Pt–Ru/C catalyst prior to adding the ethanol.

The Nafion solution used for the preparation of PEM for DMFC using EHDA LbL deposition was prepared by the mixing of 5 wt.% Nafion solution (DuPont, Wilmington, USA) and appropriated methanol (99.5 wt.%, Tianjin Kermel Chemical Reagent Co., Ltd, Tianjin, China) under magnetic stirring for 0.5 h. Two Nafion solutions with different concentrations were used for the preparation of PEM using EHDA LbL deposition in this work in order to examine their effect on the feature of the Nafion membranes. The addition of methanol was to dilute the dense Nafion solution (5 wt.%) and to reduce the stress during the film formation process which can result in the crack of the Nafion membrane during the EHDA deposition process.

2.2. EHDA deposition of catalyst suspensions and Nafion solution

The EHDA deposition device is shown in Fig. 1, which comprises of an electrohydrodynamic needle coupled together with a computer controlled X–Y movement stage and a microscopic vision system. The X–Y movement stage consists of an X–Y stepper motor driven 2-axis system. The X and Y axes are mounted directly on one another and the top of the axis accommodates a 120 mm × 120 mm table for holding ground electrode and substrate. An end of travel limit sensor is fitted on each of the axes to trigger the controller when a respective carriage reaches a limit. The 2-axis system is computer-controlled using a programmable motion controller and Labview software. The needle (inner/outer diameter of 0.4/0.7 mm) was connected to a high voltage power supply (Teslaman Technology Co., Ltd, Dalian, China) and its inlet was connected to a syringe pump (Baoding Longer Precision Pump Co., Ltd., Baoding, China) using a silicone rubber tube through which suspensions/solution were pumped. The high voltage power supply was used to apply an electric field between the needle and the ground electrode, and the syringe pump was employed to provide the hydrodynamic force to push the suspensions/solution up to the outlet of the needle. An aluminium plate with a thickness of 6 mm, serving as the ground electrode, was placed directly on the table of the X–Y movement stage and connected to earth potential. The microscopic vision system with a magnification of range of 0.7–4.5× and focal length of 320 mm was used to allow observation of the characteristics of the suspensions/solution undergoing atomization.

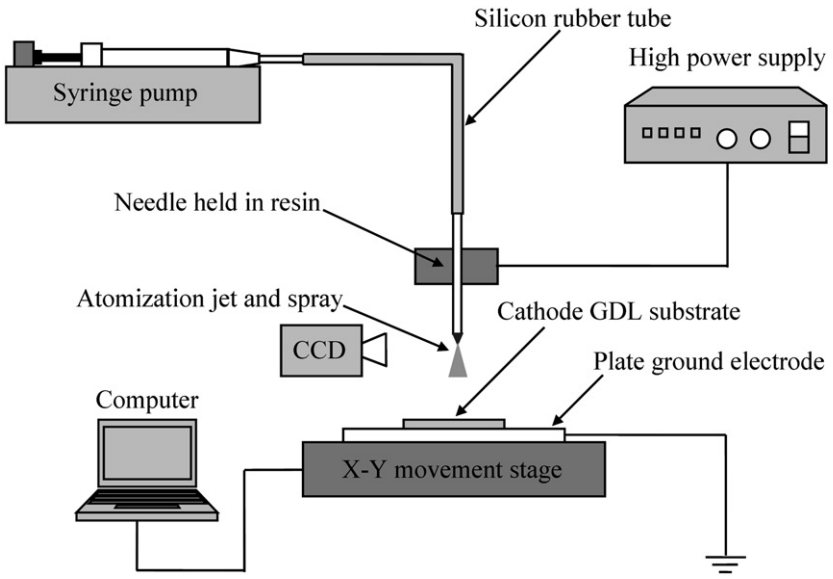

Fig. 1. Schematic representation of EHDA deposition equipment set-up.

The fabrication process of the CCM using the EHDA LbL deposition is shown in Fig. 2. The substrate, a 15 mm × 15 mm carbon paper (TGP-H-060, Toray Carbon, Japan), treated initially by dipping in a 30 wt.% PTFE solution for 1 min and coated with carbon ink to form micro-porous layer using painting process, was placed on the aluminium plate ground electrode for the EHDA LbL deposition. During the formation of the anode and cathode CLs the substrate was scanned with the *X*–*Y* movement in the *X* direction (*Y* direction step) for one layer and in the *Y* direction (*X* direction step) for each alternate layer with a travelling speed of 3.2 mm s^{-1}. The step distance (distance between two neighbouring parallel paths) of deposition was set to 0.4 mm to ensure a degree of overlap between deposited materials. During the formation of the Nafion membrane the step distance were set to 0.3 mm, and the travelling speed of 3.2 mm s^{-1} and 5.6 mm s^{-1} were tested. After every two layers of EHDA deposition of Nafion solution the film was dried at 65 °C for 3 min to remove the solvent.

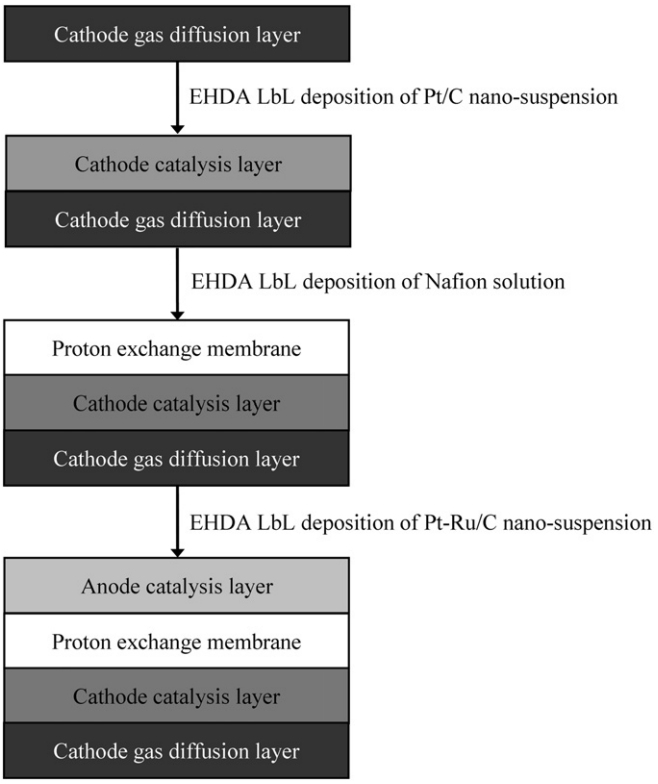

Fig. 2. Flow chart illustrating the integrated CCM preparation route using EHDA LbL deposition.

2.3. Single DMFC test

A single DMFC was assembled with the prepared integrated CCM, anode GDL, anode and cathode current collectors, anode flow field plate and cathode end plate under a pressure of 0.1 MPa. The anode GDL of the single cell was carbon paper which was treated by dipping in a 20 wt.% PTFE solution for 1 min and coated with carbon ink to form micro-porous layer using painting process. Anode and cathode current collectors were made from 400 μm thick stainless steel plate, having 's' shape methanol flow channel in anode and air breathing holes in cathode. The anode flow field plate and cathode end plate were made from 3 mm thick polymethyl methacrylate (PMMA) sheets. The anode flow field plate had a 's' shape methanol flow channel with 800 μm in width and 600 μm in depth. The active area of the cell was 15 mm × 15 mm. During the test the fuel cell ran on methanol solution which was driven by a syringe pump at a flow rate of 0.83×10^{-10} m^3 s^{-1} in the anode. The cell absorbed oxygen from the ambient air (air-breathing mechanism) in the cathode. The performance (current density–voltage and current density–power density curves) and Nyquist plot (impedance response) of the cell at the working temperature range from 20 °C to 70 °C were obtained using a DC electronic load and electrochemical station. The choose of the highest examined temperature of 70 °C is to ensure the fixing stability of the DMFC because the anode flow field plate and cathode end plate were made from PMMA which cannot tolerate high temperature. It was observed in our experiment that the distortion of the anode flow field plate and cathode end plate were likely to happen when the cell work above 70 °C, which can affect the tightness between the elements of the DMFC. The working temperature of the cell was controlled by placing the cell in a temperature programmable chamber (Dong Guan Bell Test Equipment Co., Ltd, Guangdong, China).

3. Results and discussion

3.1. EHDA deposition of catalyst layers

Fig. 3a shows a typical stable cone-jet mode formed at an applied voltage of 3 kV, a flow rate of 3.2 × 10^{-11} m^3 s^{-1} and a working distance of 5 mm using the Pt/C nano-suspension. The following deposition of anode and cathode CLs were produced under this type of stable cone-jet mode. The atomization parameters for the EHDA deposition of anode CL using Pt–Ru/C nano-suspension were the same with those for cathode CL deposition. Fig. 3b and c show the surface features of the cathode and anode CLs after 20 layers of EHDA deposition. It can be seen that the films presented porous surface feature. The average pore size was ~2 μm for the cathode CL and ~4 μm for the anode CL, which are suitable for the transport of reactants and reaction products [32]. The pore size at sub-micrometre in size can be further adjusted by the control of the working parameters of working distance and flow rate using the EHDA deposition technique, which was observed in our previous work [33]. The porous behaviour of the deposited films can be attributed to the atomize-deposited relics that were formed during the EHDA process [34]. The existing relics deposited previously can serve as an electrode for the oncoming travelling droplets because of the higher electrical field. Therefore, the atomized travelling droplets are attracted and prefer to settle above the existing relics, resulting in the porosity of the deposited films.

3.2. EHDA deposition of Nafion membrane

Fig. 4a shows the atomization mode formed at an applied voltage of 3.3 kV, a flow rate of 2.5 × 10^{-10} m^3 s^{-1} and a working distance of 15 mm using the 3.3 wt.% Nafion solution (mixing of 2 g of 5 wt.% Nafion solution and 1 g of methanol). It was found that the EHDA of Nafion solution presented a cone-jet mode with long and thick jet and less spray region compared with that of Pt/C nano-suspension. This type of long cone-jet mode can help to form dense Nafion membrane due to bigger deposited products [34]. Fig. 4b shows the Nafion membranes deposited using the 4.2 wt.% Nafion solution (mixing of 2.5 g of 5 wt.% Nafion solution and 0.5 g of methanol). The travelling speed and step distance were set at 3.2 mm s^{-1} and 0.3 mm, respectively. It was observed that large cracks were evident in the film after 20 layers EHDA deposition, caused by the high shrinkage-induced stress in the film during the drying process. These cracks in the Nafion membrane can result in the crossover of methanol solution and reduce the reaction efficiency. Therefore, dense Nafion membrane was normally used in DMFC [35]. In order to reduce the shrinkage-induced stress the concentration of the Nafion solution was decreased and the travelling speed was increased. Fig. 4c exhibited a crack-free Nafion membrane produced using 3.3 wt.% Nafion solution and at a travelling speed of 5.6 mm s^{-1}, which suggested that these are the appropriate conditions suitable for the preparation of Nafion membrane for DMFC using EHDA deposition technique.

3.3. Formation of integrated CCM

Based on the above analysis the integrated CCM was fabricated by using EHDA LbL deposition of Pt/C nano-suspension, Nafion solution and Pt–Ru/C nano-suspension in succession. The CL thickness between 10 μm and 30 μm was normally produced using decal transfer, direct coating and hot-pressed method, which can give reasonable performance of DMFC [11,36]. Depending on

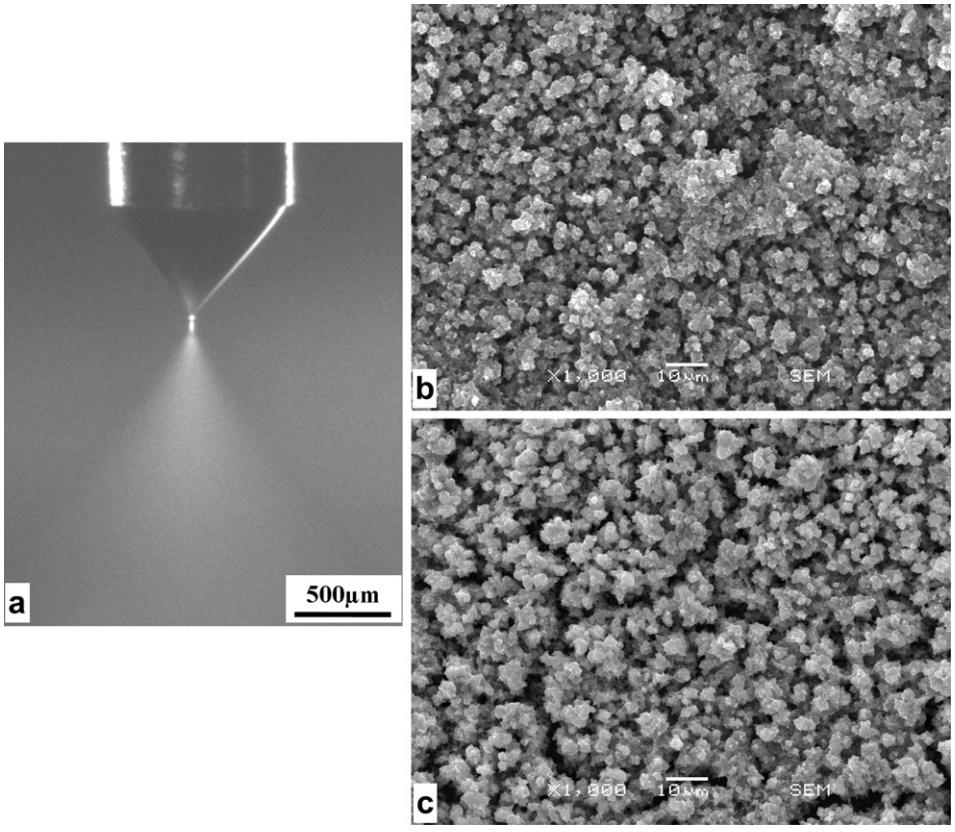

Fig. 3. A typical stable cone-jet mode of Pt/C nano-suspension (a) and scanning electron microscope micrographs showing the microstructure of the surface of the EHDA LbL deposited cathode CL (b) and anode CL (c) obtained at an applied voltage of 3 kV, a flow rate of 3.2 × 10^{-11} m^3 s^{-1} and a working distance of 5 mm.

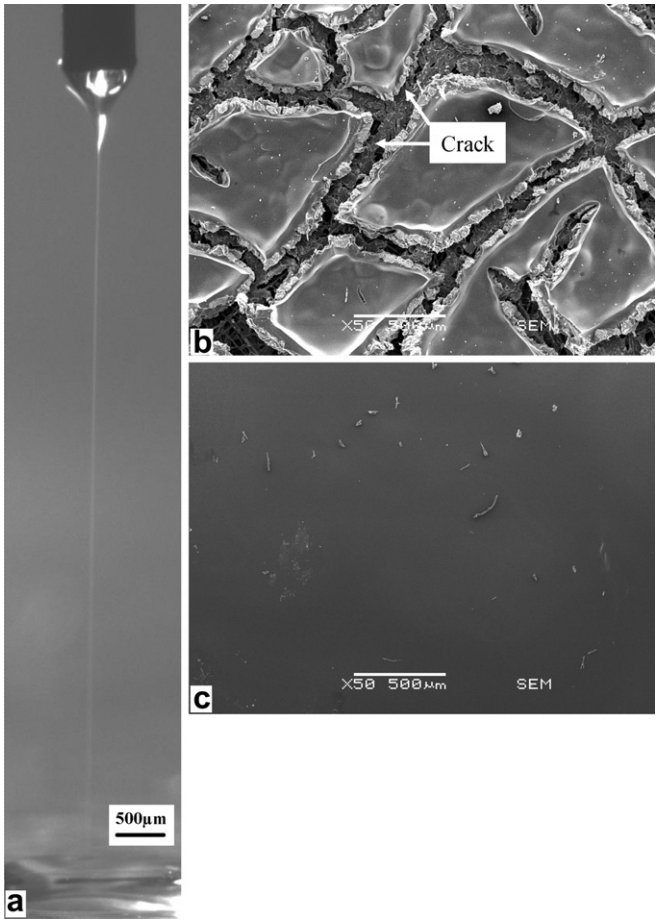

Fig. 4. A typical long cone-jet mode of Nafion solution (a) and scanning electron microscope micrographs showing the microstructure of the surface of the EHDA LbL deposited Nafion membrane produced from different concentrations of Nafion solution: (b) 4.2 wt.% and (c) 3.3 wt.%.

application reason it is very important to reduce the catalyst loadings under a level of less than 1.0 mg cm^{-2} [37]. It was also reported that the catalyst loading in cathode electrode can be lower than that in anode electrode [38,39]. Therefore, in this work the cathode and anode CLs were constructed by 20 layers EHDA LbL deposition, which can give thickness of cathode and anode CL of approximate 15 μm and 30 μm and catalyst loading of cathode (Pt) and anode (Pt–Ru) of approximate 0.4 mg cm^{-2} and 1 mg cm^{-2}. During the EHDA LbL deposition of the integrated CCM the atomization conditions were kept the same as those for the cathode and anode CLs deposition discussed in Section 3.1 and crack-free Nafion membrane deposition discussed in Section 3.2. Fig. 5 shows the cross-section of the CCM produced using the EHDA LbL deposition. It can be seen that the CCM exhibited close packed structure (Fig. 5). The catalyst electrodes have been integrated with the Nafion membrane due to the close contact between the catalyst layer and the membrane. It also can be seen that there are pore-like features present in the cathode CL, which is probably due to the infiltration behaviour of the Nafion solution into the bigger pores existing in the cathode CL during the EHDA LbL deposition of Nafion solution on the cathode CL. The infiltration of Nafion solution in the pores of cathode CL during the EHDA deposition process and the following evaporation of the solvent can enlarge the pores existed in the cathode CL. The thickness of the Nafion membrane is ~120 μm after 28 layers EHDA deposition, comparable with the commercial Nafion membrane [40].

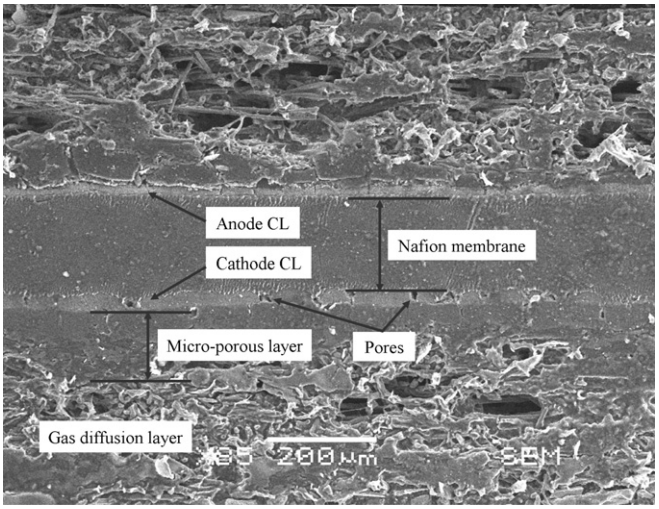

Fig. 5. Scanning electron microscope micrographs showing a typical cross-section of the integrated CCM produced using the EHDA LbL deposition.

3.4. Performance of single DMFC

The performance comparison of the DMFC with different methanol concentrations is shown in Fig. 6. The peak power density increased from 1.4 mW cm^{-2} to 1.7 mW cm^{-2} when the concentration of methanol increased from 1 M to 3 M. This is because more methanol molecules can be catalyzed on the surface of catalyst when using higher concentrated methanol. However, the peak power density dropped to 1.1 mW cm^{-2} and 0.9 mW cm^{-2} when the fuel concentration was 4 M and 5 M, which is mainly due to the higher methanol crossover when the fuel concentration increased [41]. The effect of the potential generated from methanol crossover exceeded that of the concentration of methanol molecules close to catalyst, which resulted in the decrease of cell performance at higher methanol concentration above 3 M. Therefore, the 3 M methanol is the appropriate concentration using this DMFC under this testing system. The following examinations on the polarization behaviour, impedance response and life test of the cell were conducted using the 3 M methanol.

Fig. 7 illustrates the current density–voltage and current density–power density curves of the DMFC assembled with the

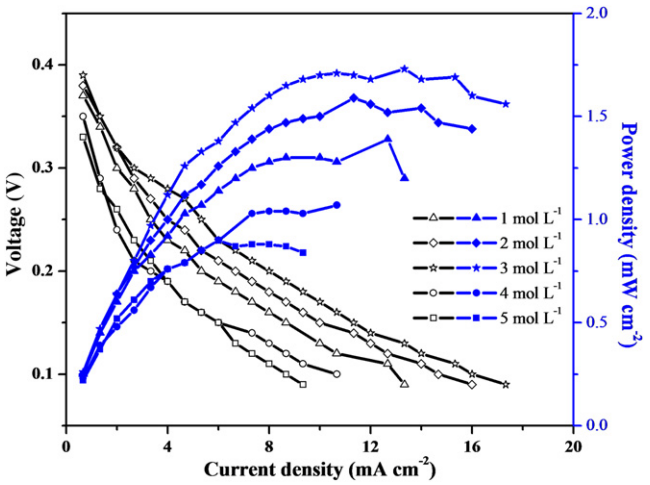

Fig. 6. Current density–voltage and current density–power density curves of the single cell at different methanol concentrations.

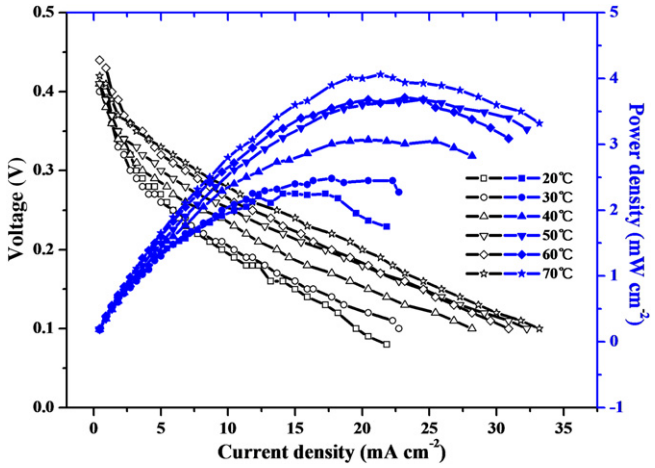

Fig. 7. Current density–voltage and current density–power density curves of the single cell at different temperatures.

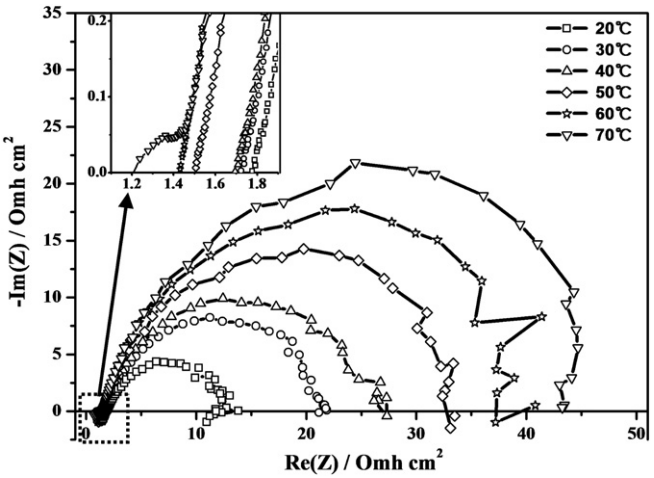

Fig. 9. Impedance curves of the single cell at different temperatures.

EHDA LbL deposited integrated CCM at different temperatures. It can be seen that the cell performance increased significantly between 20 °C and 50 °C, which can be attributed to the high activity of the thermal motion of gas (O_2) molecule, catalytic reaction in both cathode and anode CLs and proton transfer when the temperature rose. Within this range, the reaction gas of O_2 was sufficient and the redox reactions at cathode and anode CLs increased continuously, so the power density increased with higher temperature. When the temperature grew from 50 °C to 70 °C, the increase level of the cell performance decreased compared with that between 20 °C and 50 °C. The escalating activity of reaction in the cathode CL with higher temperature resulted in larger amount of water, which left lower reaction space of O_2 and larger gas-phase transport resistance. Therefore, the improvement of the cell performance at higher temperature increasing region (50 °C–70 °C) was lower than that at the lower temperature region (20 °C–50 °C). The peak power density of this cell was 4 mW cm^{-2} at 70 °C under the test condition of active methanol solution in the anode and passive oxygen breath from the ambient air in the cathode. This lower performance behaviour of the cell is mainly due to the lower Pt and Pt–Ru catalyst loading and passive oxygen breath from the ambient air in the cathode.

Fig. 8 shows the crossover current density versus applied voltage at different temperatures, which was measured by supplying methanol solution in anode and N_2 in cathode. When the applied voltage increased the crossover current increased and approached a plateau of limiting current at ~0.9 V. The methanol diffusion coefficient (D_{meth}) at different temperatures can be estimated using the limiting currents obtained from Fig. 8 and the following equation [42].

$$D_{meth} = \frac{I_{crossover}/A}{nFC_{meth}/d_{mem}}$$

Where $I_{crossover}$ is the limiting methanol crossover current, A is the geometrical active area of the electrode which is 2.25 cm^2 for this cell, C_{meth} is the concentration of methanol within the membrane which is 3.8×10^{-4} mol cm^{-3} inferred from Qi and Kaufman's work [42], d_{mem} is the thickness of the Nafion membrane which is 120 μm in the integrated CCM produced in this work, n is the number of electrons involved in the oxidation of each methanol molecule which is 6 when we assume the methanol is completely oxidized to CO_2 and F is the Faraday constant which is 96487 C mol^{-1}.

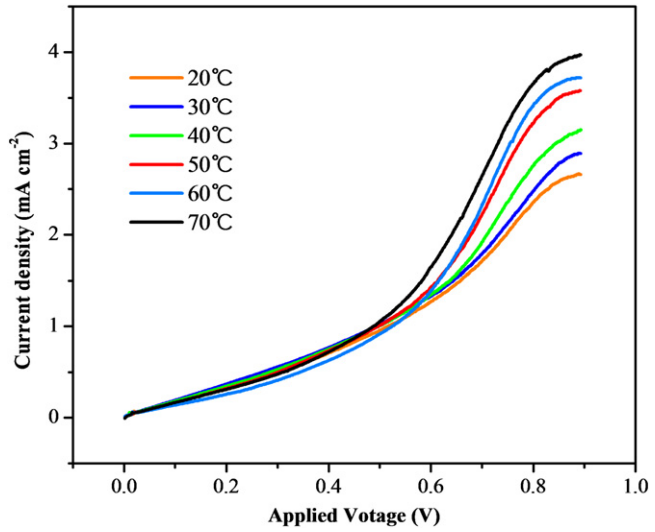

Fig. 8. Crossover current density–applied voltage of the single cell at different temperatures.

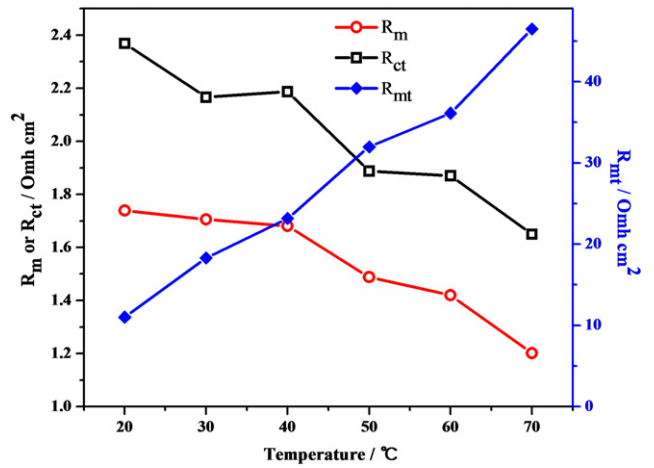

Fig. 10. The fitting curves of the ohmic resistance, charge transfer resistance and mass transfer resistance of the single cell from the measured impedances at different temperatures.

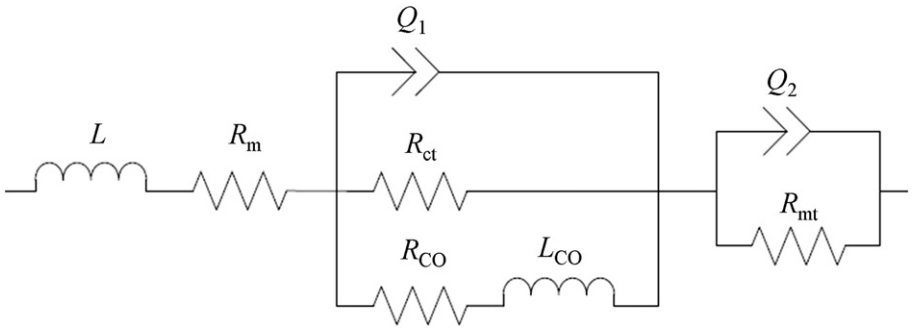

Fig. 11. Equivalent circuit model for the modelling of the single cell impedance.

Therefore, according to the above equation and Fig. 8 the methanol diffusion coefficient (D_{meth}) at the temperature range from 20 °C to 70 °C was 1.50×10^{-7}, 1.61×10^{-7}, 1.77×10^{-7}, 2.0×10^{-7}, 2.12×10^{-7} and 2.22×10^{-7} $cm^2\ s^{-1}$, respectively. It can be seen that the methanol diffusion coefficient increased with higher temperature, which is mainly due to the softening of the fluorinated chain in the Nafion membrane leading to an increase of membrane diffusivity at high temperature [41]. It was also found that the increase value of the methanol diffusion coefficient between 40 °C and 50 °C ($\sim 0.25 \times 10^{-7}$ $cm^2\ s^{-1}$) is about double of other 10 °C temperature increase steps ($\sim 0.1 \times 10^{-7}$ $cm^2\ s^{-1}$). This means that higher methanol crossover and higher overpotential will happen when a temperature is above 50 °C, which will also help to reduce the cell performance at a greater degree at a temperature higher than that. Therefore, this is another reason for the lower improvement of the cell performance at higher temperature increasing region from 50 °C to 70 °C compared with the region from 20 °C to 50 °C (Fig. 7).

The impedance response curves of the single cell assembled with the EHDA deposited CCM at different temperature are shown in Fig. 9, which was obtained at the frequency range from 0.01 Hz to 100 kHz. The fitting curves including the ohmic resistance, charge transfer resistance and mass transfer resistance from the impedance measurement results (Fig. 9) are shown in Fig. 10 which was obtained based on the equivalent circuit model (Fig. 11) presented by Seo and Lee [43] and Jin et al. [44]. In the equivalent circuit model (Fig. 11), R_m is the ohmic resistance, R_{ct} is the charge transfer resistance, R_{mt} is the mass transfer resistance, L is the pseudoinductance induced by the outside circuits and test equipments, Q_1 and Q_2 express the charge and discharge process of the double layer capacity of the anode and cathode, resistance of R_{CO} and low frequency impedance of L_{CO} express the relaxation process of the CO product in the anode electrode.

It is known that the intersection point of the arc and Re(Z) axis in the impedance curves represents the total ohmic resistance of the cell and the arc at low frequency mainly illustrates the gas-phase transport resistance. It was observed that the ohmic resistance (R_m) decreased from 1.8 to 1.2 Ω cm^2 when the temperature increased from 20 °C to 70 °C (Figs. 9 and 10). The behaviour of lower ohmic resistance with higher temperature was also observed in Seo and lee's work [43]. It was also found that the charge transfer resistance (R_{ct}) decreased with the increase of temperature (Fig. 10), which is mainly due to the high activity of the electron and proton transfer when the temperature rose. These are all consistent with that of the current density–voltage and current density–power density curves studied in Fig. 7, where the performance of the cell enhanced when the temperature rose. However, the impedance arc became larger and the mass transfer resistance (R_{mt}) became higher with higher temperature (Figs. 9 and 10). This is because that the fast oxidation reaction on the cathode catalyst layer induced larger amount of water under the passive air breath environment in cathode, which can affect gas transport in the cathode GDL and bring about larger gas-phase transport resistance. This is also in agreement with the current density–voltage and current density–power density curves studied in Fig. 7, in which the increase level of the cell performance decreased at higher temperature range.

3.5. Lift test of single DMFC

The result of an 85 h life test of the DMFC at 10 mA cm^{-2} and 30 °C is shown in Fig. 12. During the life test, the continuous discharge was interrupted by the replacement of full methanol syringe, which causes spikes on the single cell voltage versus time plot (Fig. 12). It was found that the cell can recover its initial performance within the 15 h duration test. A degradation rate of ~ 1.6 mV h^{-1} was observed in the every continuous discharge operation duration. Fig. 13 shows the cross-section of the MEA after 85 h life test. It was observed that the anode GDL delaminated from the membrane after the life test compared with the compact MEA before the test (Fig. 5). This is a reason of the reduction of the cell performance after the life test (Fig. 12) because the delamination can reduce the proton and electron transport and result in the lower performance of the cell. The delamination of the anode electrode side is due to the water swelling property of Nafion membrane and poor bonding between the anode GDL and Nafion membrane, which was also observed in our previous work [10]. The

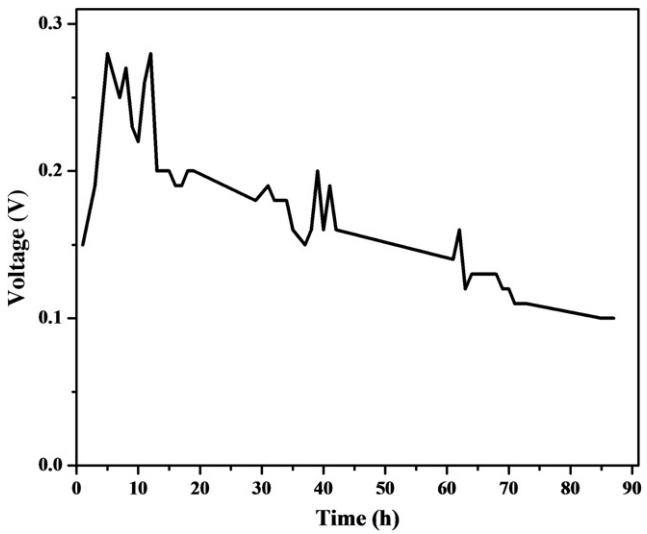

Fig. 12. Life test of the single cell.

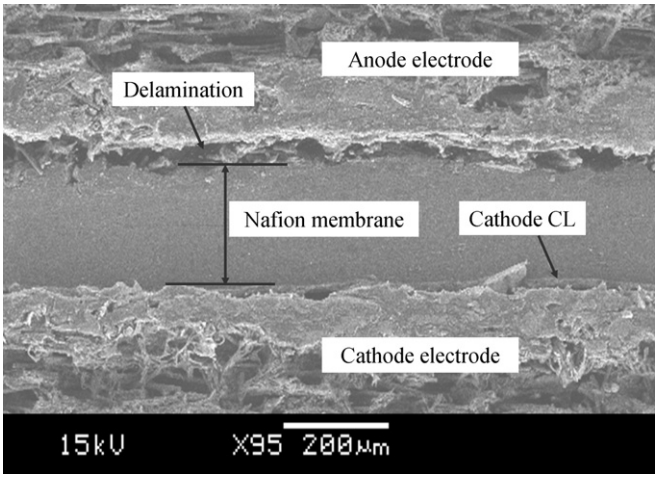

Fig. 13. Scanning electron microscope micrographs showing a typical cross-section of the EHDA LbL deposited integrated CCM after 85 h life test.

anode GDL was directly pressed on the Nafion membrane to form anode electrode side. The bonding force provided by this direct pressed method cannot suffer the swelling of the membrane during the working of the DMFC, then the delamination happened.

However, it was also observed that the cathode electrode side still remains the compact structure after the life test (Fig. 13) compared with the anode electrode side. The cathode CL and Nafion membrane were fabricated by successively EHDA LbL deposition of Pt/C nano-suspension and Nafion solution on carbon paper substrate. The droplet atomized by EHDA process from Pt/C nano-suspension are nanometres in size and thus the cathode CL was formed by the deposition of nano-structures LbL on the porous GDL [33], which can give well-knit contact between CL and GDL. Moreover, the EHDA initially deposited Nafion membrane on the cathode CL was liquid form and will perform a drying process in order to remove the solvent in the Nafion membrane. Consequently, some Nafion solution will infiltrate in the cathode CL during the EHDA deposition process and become dry Nafion membrane after the drying process. The Nafion membrane infiltrated in the CL can provide firm link between the cathode CL and Nafion membrane, which can improve the bonding between the CL and Nafion membrane. Therefore, the cathode electrode side produced by the EHDA LbL deposition technique can contribute better boning behaviour compared with the anode electrode side assembled by the direct pressed method, resulting in the compact structure after the life test. It is noted that this cathode electrode side with compact feature after 85 h life test is also an improvement compared with the delamination behaviour in the CCM produced by the hot-pressed method after 75 h life test in our previous work [10].

4. Conclusions

The use of the EHDA LbL deposition technique for depositing Pt/C nano-suspension, Nafion solution and Pt–Ru/C nano-suspension to form integrated CCM was aptly demonstrated. The integrated CCM was prepared by EHDA LbL depositing 20 layers of Pt/C nano-suspension, 28 layers of Nafion solution and 20 layers of Pt–Ru/C nano-suspension, respectively. It was found that the integrated CCM exhibited close packed structure and the catalyst electrodes have been integrated with the Nafion membrane. It also can be seen that there are pore-like features in the CL using this LbL deposition technique, which is a weakness compared with the painting and hot-pressed method. Further improvement on the optimization of the working parameters of the EHDA LbL deposition need to be conducted. After an 85 h life test, it was observed that the EHDA LbL deposited cathode electrode side of the integrated CCM still presented well compact feature. The cell performance increased when the temperature rose, and the enhancement level of the cell performance was more significant at lower temperature range than that at higher temperature. The impedance arcs and its fitting curves show that the impedance arc became larger and the mass transfer resistance became higher with higher temperature, that is, the gas-phase transport resistance became larger as the temperature rose. The methanol crossover test shows that the cell presented higher increase level of methanol crossover between 40 °C and 50 °C than other 10 °C temperature increase steps. The peak power density of 4 mW cm^{-2} at 70 °C was obtained for the cell assembled with the EHDA LbL deposited CCM. The performance can be improved further by increasing the Pt and Pt–Ru catalyst loading through the increase of the EHDA deposition layers and improving the cell working conditions using the active oxygen breath instead of the passive air breath in the cathode. The fabrication of the integrated CCM using EHDA LbL deposition provides a new, effective and promising manufacturing route for fuel cell device.

Acknowledgements

This research is supported by the National Natural Science Foundation of China (No. 50905027, No. 5175076), Specialized Research Fund for the Doctoral Program of Higher Education of China (No. 20090041120041), Fundamental Research Funds for the Central Universities (No. DUT12JB08) and the Scientific Research Foundation for the Returned Overseas Chinese Scholars, State Education Ministry.

References

[1] X. Ren, P. Zelenay, S. Thomas, J. Davey, S. Gottesfeld, J. Power Sources 86 (2000) 111–116.
[2] A. Faghri, Z. Guo, Appl. Therm. Eng. 28 (2008) 1614–1622.
[3] M. Carmoa, V.A. Paganina, J.M. Rosolenb, E.R. Gonzaleza, J. Power Sources 142 (2005) 169–176.
[4] T. Frey, M. Linardi, Electrochim. Acta 50 (2004) 99–105.
[5] Y.J. Zhang, C. Wang, N.F. Wan, Z.X. Liu, Z.Q. Mao, Electrochem. Commun. 9 (2007) 667–670.
[6] M. Prasanna, H.Y. Ha, E.A. Cho, S.A. Hong, I.H. Oh, J. Power Sources 137 (2004) 1–8.
[7] K.H. Kim, K.Y. Lee, S.Y. Lee, E. Cho, T.H. Lim, H.J. Kim, S.P. Yoon, S.H. Kim, T.W. Lim, J.H. Jang, Int. J. Hydrog. Energy 35 (2010) 13104–13110.
[8] L. Xiong, A. Manthiram, Electrochim. Acta 50 (2005) 3200–3204.
[9] T. Suzuki, Y. Tabuchi, S. Tsushima, S. Hirai, Int. J. Hydrog. Energy 36 (2011) 5479–5486.
[10] J.G. Liu, Z.H. Zhou, X.S. Zhao, Q. Xin, G.Q. Sun, B.L. Yi, Phys. Chem. Chem. Phys. 6 (2004) 134–137.
[11] D. You, Y. Lee, H. Cho, J.H. Kim, C. Pak, Int. J. Hydrog. Energy 36 (2011) 5096–5103.
[12] G. Decher, Science 277 (1997) 1232–1237.
[13] S.P. Jiang, Z. Liu, Z.Q. Tian, Adv. Mater. 18 (2006) 1068–1072.
[14] K. Ariga, J.P. Hill, Q. Ji, Phys. Chem. Chem. Phys. 9 (2007) 2319–2340.
[15] M. Michel, A. Taylor, R. Sekol, P. Podsiadlo, P. Ho, N. Kotov, L. Thompson, Adv. Mater. 19 (2007) 3859–3864.
[16] A. Jaworek, A. Krupa, J. Aerosol Sci. 30 (1999) 873–893.
[17] J. Zeleny, Phys. Rev. 3 (1914) 69–91.
[18] S.N. Jayasinghe, M.J. Edirisinghe, Mater. Res. Innov. 7 (2003) 62–64.
[19] A. Jaworek, J. Mater. Sci. 42 (2007) 266–297.
[20] M. Cloupeau, B. Prunetfoch, J. Aerosol Sci. 25 (1994) 1021–1036.
[21] G. Taylor, Proc. R. Soc. Lond. 280 (1964) 383–397.
[22] A.R. Jone, K.C. Thong, J. Phys. D Appl. Phys. 4 (1971) 1159.
[23] I.G. Loscertales, A. Barrero, I. Guerrero, R. Cortijo, M. Marquez, A.M. Ganan-Calvo, Science 295 (2002) 1695–1698.
[24] M.J. Edirisinghe, S.N. Jayasinghe, Int. J. Appl. Ceram. Technol. 1 (2004) 140–145.
[25] B.Y. Tay, J.R.G. Evans, M.J. Edirisinghe, Int. Mater. Rev. 48 (2003) 341–370.
[26] A. Jaworek, A.T. Sobczyk, J. Electrost. 66 (2008) 197–219.
[27] F. Bortolani, R.A. Dorey, Adv. Appl. Ceram. 108 (2009) 332–337.

[28] S.A. Rocks, D. Wang, D. Sun, S.N. Jayasinghe, M.J. Edirisinghe, R.A. Dorey, J. Electroceram. 19 (2007) 287–293.
[29] Z. Ahmad, M. Rasekh, M. Edirisinghe, Macromol. Mater. Eng. 295 (2010) 315–319.
[30] M. Rasekh, Z. Ahmad, R. Day, A. Wickam, M. Edirisinghe, Adv. Eng. Mater. 13 (2011) 296–305.
[31] M.S. Wilson, S. Gottesfeld, J. Electrochem. Soc. 139 (1992) 28–30.
[32] M.C. Tucker, M. Odgaard, P.B. Lund, S. Yde-Andersen, J.O. Thomasa, J. Electrochem. Soc. 152 (2005) 1844–1850.
[33] D. Wang, H. Duan, J. Liang, C. Liu, Micro Nano Lett. 7 (2012) 235–239.
[34] D. Wang, S.A. Rocks, R.A. Dorey, J. Eur. Ceram. Soc. 32 (2012) 1651–1658.
[35] M.A. Smit, A.L. Ocampo, M.A. Espinosa-Medina, P.J. Sebastián, J. Power Sources 124 (2003) 59–64.
[36] H. Tang, S. Wang, S. Jiang, M. Pan, J. Power Sources 170 (2007) 140–144.
[37] H. Liu, C. Song, L. Zhang, J. Zhang, H. Wang, D.P. Wilkinson, J. Power Sources 155 (2006) 95–110.
[38] Z. Shao, W. Lin, F. Zhu, P.A. Christensen, M. Li, H. Zhang, Electrochem. Commun. 8 (2006) 5–8.
[39] K.Y. Song, H.K. Lee, H.T. Kim, Electrochim. Acta 53 (2007) 637–643.
[40] J.G. Liu, T.S. Zhao, Z.X. Liang, R. Chen, J. Power Sources 153 (2006) 61–67.
[41] A. Casalegno, P. Grassini, R. Marchesi, Appl. Therm. Eng. 27 (2007) 748–754.
[42] Z. Qi, A. Kaufman, J. Power Sources 110 (2002) 177–185.
[43] S.H. Seo, C.S. Lee, Energy Fuels 22 (2008) 1204–1211.
[44] B. Jin, S. Wang, X. Xie, J. Guo, L. Qi, J. Wang, J. Tsinghua Univ. 48 (2008) 2107–2110.